INTERNATIONAL JOURNAL FOR NUMERICAL AND ANALYTICAL METHODS IN GEOMECHANICS
Int. J. Numer. Anal. Meth. Geomech., 2000; **24**:305–325

Prediction of the initial normal stress in piles and anchors constructed using expansive cements

C. M. Haberfield*†

Department of Civil Engineering, Monash University, Clayton, 3168, Australia

SUMMARY

Uses for expansive cements and additives have extended well beyond off-setting the shrinkage characteristics of grout and concrete to include enhancement of rock anchor and pile performance, providing an alternative form of connection for tubular members in off-shore structures and as an excavation tool in open-pit mines. In each case, the design rules governing the quantity of expansive additive to be used are based on guesswork or empiricism. This paper presents analytical solutions for estimating the degree of expansion and the level of normal stress developed for a range of different boundary conditions and expansive additive contents. The expansion process is modelled as a thermal expansion and is governed by one parameter that depends on the type of expansive additive and its dosage. Simple laboratory procedures for determining this property are outlined. Predictions from the analytical solutions are compared with laboratory experiments. Copyright © 2000 John Wiley & Sons, Ltd.

KEY WORDS: expansive cement; piles; anchors; rock; initial normal stress; analytical solution

INTRODUCTION

After cement grout (or concrete) sets and is allowed to dry, it undergoes a sometimes-destructive phenomenon known as drying shrinkage. As cement grout is relatively weak in tension, especially at a young age, if it is restrained from shrinking (e.g. by reinforcement, friction, connections or other boundary conditions) it will crack, often causing severe structural damage. Expansive cements and additives were basically developed to minimize this drying shrinkage.

The use of expansive cements has been largely restricted to shrinkage compensating rather than self-stressing applications. The difference between the two is essentially the amount of expansion (or potential expansion) that takes place. Shrinkage-compensating cement will expand no more than the magnitude of the drying shrinkage of the grout. A self-stressing cement will expand (if not restricted) more, so that the net volume after expansion and shrinkage is greater than the initial volume.

Recently, both industry and researchers have recognized the possible benefits that can be obtained using self-stressing cements. These include enhancing the performance of anchors

* Correspondence to: Dr. C. M. Haberfield, Department of Civil Engineering, Monash University, Clayton, 3168, Australia
† E-mail: chris.haberfield@eng.monash.edu.au

Contract/grant sponsor: Australian Research Council

Received 31 January 1999
Revised 26 May 1999

and piles in rock[1,2] and as a more efficient and reliable method of connecting tubular members in off-shore construction. Both applications essentially utilize the expansive cement in the same way.

When an anchor or pile is constructed with expansive cement, the expansion process causes the concrete of the pile (or anchor) to expand against the stiffness of the surrounding rock (Figure 1). Since the rock resists this expansion, a normal stress is generated across the pile/rock interface. As this stress is induced before axial loading of the pile, it is referred to as the initial normal stress. For piles and anchors constructed using normal portland cement the initial normal stress is relatively low. However, during axial loading, slip occurs and the normal stress is increased significantly above the initial value due to the dilation of the rough pile/rock interface.[1] Any increase in normal stress increases the frictional resistance of the pile, thereby leading to enhanced performance. For relatively smooth piles, the dilation and therefore normal stress generated during loading is relatively small. As a result pile capacity is also low. The potential for increasing the capacity of such piles and anchors through generating substantially higher initial normal stresses is therefore high. Haberfield *et al.*[1] investigated the influence of increasing levels of initial normal stress by using expansive cements. They showed that increases in pile and anchor capacity of up to 300 per cent can be achieved with expansive cements.

Grundy and Foo[3] proposed that tubular steel connections could be made by utilizing expansive cements. They showed that an extremely strong joint could be manufactured by placing one tube inside another and filling the annulus between the two tubes with expansive cement grout (Figure 2). The grout tries to expand against the stiffness of the two tubes, thereby generating very large normal stresses that lock the two tubes together.

In both applications the expansion of the grout in a confined space leads to the generation of normal stresses which in turn leads to enhanced performance. However, the degree of normal

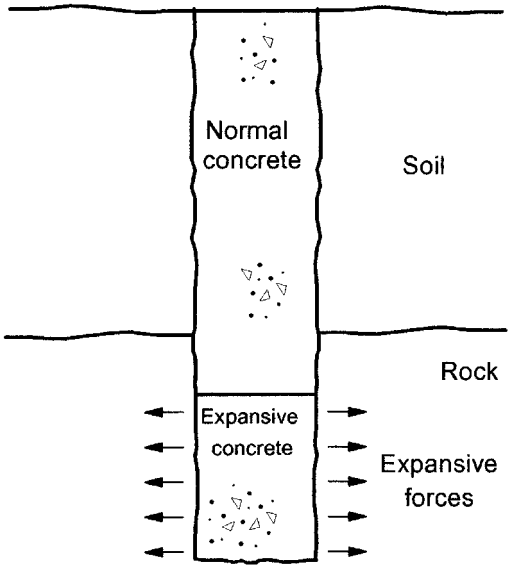

Figure 1. Enhancement of pile capacity in rock using expansive cement

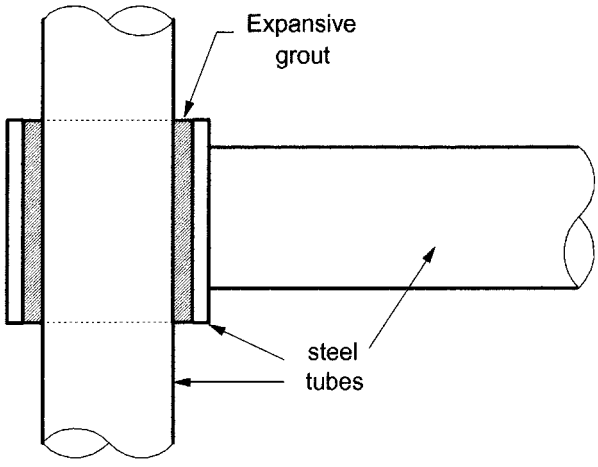

Figure 2. Enhancement of performance of tubular steel connections using expansive cement

stress generated depends on the level of the confinement and the concentration of expansive additive. If confinement is low, then the expansive grout will expand freely and result in severe loss of grout strength, stiffness and integrity. However, for relatively high levels of confinement, the expansion of the grout is severely restricted, resulting in high levels of normal stress and increased grout strength.

The difficulty arises in determining for any given application if the confinement is adequate to ensure integrity of the grout, and the level of normal stress that can be generated for a given expansive additive content. By modelling the chemical expansion process as a thermal expansion, this paper develops theoretical solutions for the performance of expansive grouts subject to a number of common boundary constraints. The theoretical solution requires the estimation of the expansive potential, ε^{E}, of the grout. This is analagous to a thermal coefficient of expansion and can be readily determined from a simple laboratory test. This paper does not consider the long-term effects of creep which may reduce the amount of normal stress developed.

ELASTIC CAVITY EXPANSION

The applications mentioned above all involve the forced expansion of a cylindrical cavity. Cross-sections of a pile, an anchor and a tubular joint are shown in Figure 3. For the case of a pile in rock (Figure 3(a)), the expansive grout forms a long cylindrical body with its outer boundary surrounded by a rock mass of infinite extent. The rock bolt (Figure 3(b)) is similar to the pile, but has also an inner cylindrical boundary formed by the steel bolt or tendon. The tubular joint (Figure 3(c)) has inner and outer boundaries formed by steel tubes of finite wall thickness. In each case, the grout is restrained from expanding by these inner and outer boundaries at radii of r_i and r_o, respectively. For purposes of analysis, these inner and outer boundaries can be replaced by normal stiffness K_i and K_o, respectively. As will be shown, due to yielding of the inner and outer boundaries, K_i and K_o are not necessarily constant but may vary with the amount of expansion.

Expansion of the grout must force a change in the position of the inner and outer boundaries. The axi-symmetric displacement of these boundaries implies that a reaction stress will be

generated to off-set the expansion. These reaction stresses are normal to the surface of the grout and are denoted p_i and p_o for inner and outer surfaces of the grout, respectively. This boundary value problem can be idealized as shown in Figure 4(a). Note that both p_i and p_o are assumed to be compressive. Since the thickness of the grout in each application is small compared to the out-of-plane direction (i.e. the length of the pile, anchor or joint), plane strain conditions have been assumed.

If it is assumed that the grout remains elastic and that it expands evenly in all in-plane directions then the total expansion of the grout in each of the orthogonal directions r, θ and z can

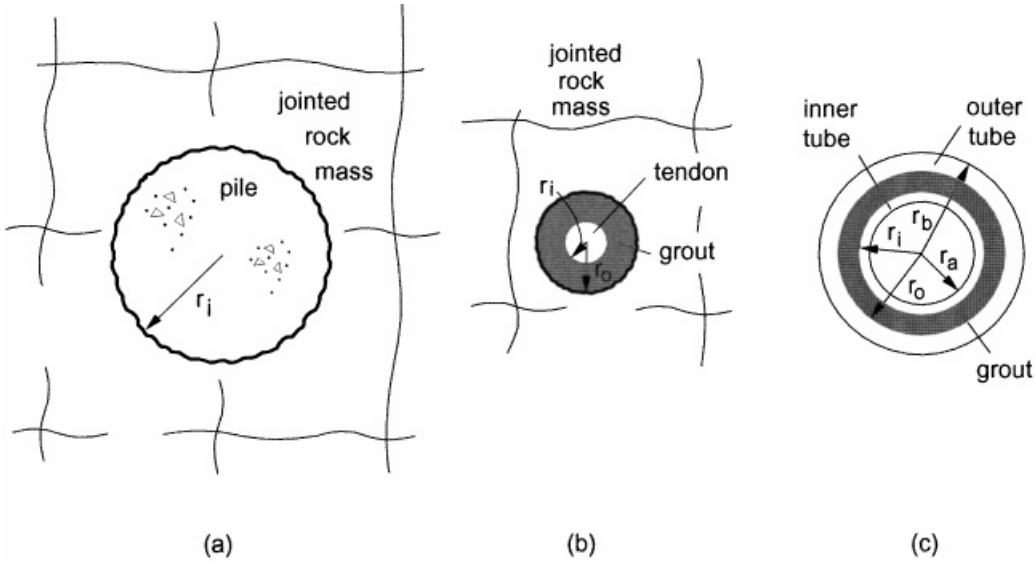

Figure 3. Cross-sections of (a) pile, (b) rock anchor and (c) tubular joint

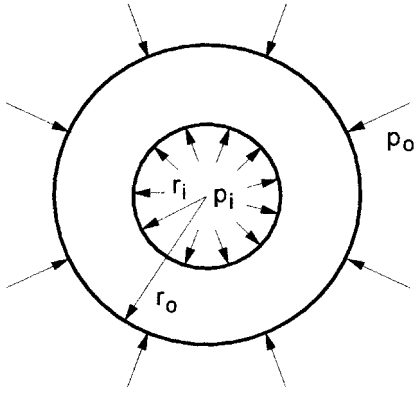

Figure 4. Idealization of general cavity expansion problem

be determined from

$$\varepsilon^{\mathrm{T}}_{r,\theta,z} = \varepsilon^{\mathrm{S}}_{r,\theta,z} + \varepsilon^{\mathrm{E}} \tag{1}$$

where $\varepsilon^{\mathrm{T}}_{r,\theta,z}$ are the total strains in each direction, ε^{E} is the expansive potential or the strain due to the chemical expansion process and $\varepsilon^{\mathrm{S}}_{r,\theta,z}$ are the strains in each direction due to any stresses that are applied.

From Hookes law,

$$\varepsilon^{\mathrm{S}}_{r,\theta,z} = \frac{1}{E_{\mathrm{g}}}\left(\sigma_{r,\theta,z} - v_{\mathrm{g}}(\sigma_{\theta,z,r} - \sigma_{z,r,\theta})\right) \tag{2}$$

where $\sigma_{r,\theta,z}$ are the stress changes in the r, θ and z directions, respectively, and E_{g} and v_{g} are the elastic Young's modulus and Poisson's ratio of the grout, respectively.

Substituting equation (2) into equation (1) and applying the plane strain condition ($\varepsilon^{\mathrm{T}}_z = 0$) leads to

$$\sigma_z = -\varepsilon^{\mathrm{E}} E_{\mathrm{g}} + v_{\mathrm{g}}(\sigma_r + \sigma_\theta) \tag{3}$$

Substituting for σ_z gives

$$\varepsilon^{\mathrm{T}}_{r,\theta} = \frac{(1 - v_{\mathrm{g}})(1 + v_{\mathrm{g}})}{E_{\mathrm{g}}}\left(\sigma_{r,\theta} - \frac{v_{\mathrm{g}}}{1 - v_{\mathrm{g}}}\,\sigma_{\theta,r}\right) + (1 + v_{\mathrm{g}})\,\varepsilon^{\mathrm{E}} \tag{4}$$

and solving for σ_r and σ_θ

$$\sigma_{r,\theta} = \frac{E_{\mathrm{g}}(1 - v_{\mathrm{g}})}{(1 - 2v_{\mathrm{g}})(1 + v_{\mathrm{g}})}\left(\varepsilon^{\mathrm{T}}_{r,\theta} + \frac{v_{\mathrm{g}}}{1 - v_{\mathrm{g}}}\,\varepsilon^{\mathrm{T}}_{\theta,r} - \left(\frac{1 + v_{\mathrm{g}}}{1 - v_{\mathrm{g}}}\right)\varepsilon^{\mathrm{E}}\right) \tag{5}$$

Enforcing the equilibrium and strain displacement relationships for small strain

$$\frac{\mathrm{d}\sigma_r}{\mathrm{d}r} + \frac{\sigma_r - \sigma_\theta}{r} = 0, \quad \varepsilon_r = \frac{\mathrm{d}U_r}{\mathrm{d}r}, \quad \varepsilon_\theta = \frac{U_r}{r} \tag{6}$$

where U_r is the radial displacement at radius r, and substituting for σ_r and σ_θ leads to the following differential equation:

$$\frac{\mathrm{d}^2 U_r}{\mathrm{d}r^2} + \frac{1}{r}\frac{\mathrm{d}U_r}{\mathrm{d}r} - \frac{U_r}{r^2} - \left(\frac{1 + v}{1 - v}\right)\frac{\mathrm{d}\varepsilon^{\mathrm{E}}}{\mathrm{d}r} = 0 \tag{7}$$

Solving for the general solution

$$U_r = A_{\mathrm{g}} r + \frac{B_{\mathrm{g}}}{r} + \left(\frac{1 + v_{\mathrm{g}}}{1 - v_{\mathrm{g}}}\right)\frac{1}{r}\int_{r_{\mathrm{i}}}^{r} \varepsilon^{\mathrm{E}} r\,\mathrm{d}r \tag{8}$$

where A_g and B_g are constants of integration. Applying the boundary conditions at $r = r_i$, $\sigma_r = -p_i$ and $r = r_o$, $\sigma_r = -p_o$ (taking tensile stresses as positive) and solving gives

$$A_g = (1 - 2v_g)\frac{B_g}{r_i^2} - \frac{p_i}{\lambda_g} \tag{9}$$

$$B_g = \frac{r_i^2 r_o^2}{r_o^2 - r_i^2}\left[\frac{p_i - p_o}{\lambda_g(1 - 2v_g)} + \left(\frac{1 + v_g}{1 - v_g}\right)\frac{I_{r_i}^{r_o}}{r_o^2}\right] \tag{10}$$

where

$$\lambda_g = \frac{E_g}{(1 - 2v_g)(1 + v_g)} \tag{12}$$

and

$$I_{r_i}^{r_o} = \int_{r_i}^{r_o} \varepsilon^E r \, dr \tag{13}$$

Note that for the special case of a solid grout cylinder (e.g. pile) where $r_i = 0$, $B_g = 0$ and

$$A_g = \frac{(1 + v_g)(1 - 2v_g)}{(1 - v_g)}\frac{I_0^{r_o}}{r_o^2} - \frac{p_o}{\lambda_g}$$

Finally, substituting for strains in equation (5) leads to the following equations for general displacements and stresses at radius r within the expanding grout:

$$U_r = A_g r + \frac{B_g}{r} + \left(\frac{1 + v_g}{1 - v_g}\right)\frac{1}{r} I_{r_i}^{r} \tag{14}$$

$$\sigma_r = \lambda_g\left[A_g - \frac{B_g}{r^2}(1 - 2v_g) - \frac{I_{r_i}^{r}}{r^2}\frac{(1 + v_g)(1 - 2v_g)}{(1 - v_g)}\right] \tag{15}$$

$$\sigma_\theta = \lambda_g\left[A_g + \frac{B_g}{r^2}(1 - 2v_g) - \frac{I_{r_i}^{r}}{r^2}\frac{(1 + v_g)(1 - 2v_g)}{(1 - v_g)}\right] \tag{16}$$

and $I_{r_i}^{r} = \int_{r_i}^{r} \varepsilon^E r \, dr$.

The integral $I_{r_i}^{r}$ is dependent on the quantity and type of expansive cement used, the stresses developed and on the total volume of grout per unit length. Methods for estimating its value are discussed in detail later in this paper.

It has been assumed that the expansive grout remains elastic throughout the expansion process. This assumption appears to be reasonable given the likely high levels of confinement. However, there may be circumstances in which the grout yields. The solution to this problem is beyond the scope of this paper.

DETERMINATION OF CONFINING STRESSES AND STIFFNESSES

The stresses, p_i and p_o that act on the inner and outer boundaries of the expanding grout annulus depend on the stiffness K_i and K_o of the surrounding material. Several different cases can be identified.

Inner and outer boundary—linear elastic

The inner boundary of the grout annulus can consist of either a solid cylinder (as in a rock anchor) or a hollow tube (as in a tubular connection). The more general case of the hollow tube is depicted in Figure 3(c). The solution to this problem (assuming that the tube remains elastic) is analagous to the problem of the expanding grout annulus described above. By substituting for the appropriate dimensions and tube material properties in equations (9)–(16), and setting $p_i = 0$ and $\varepsilon^E = 0$ the following equations, which model the elastic behaviour of the inner tube can be derived.

$$U_r = A_i r + \frac{B_i}{r} \tag{17}$$

$$\sigma_r = \lambda_i \left[A_i - \frac{B_i}{r^2} (1 - 2\nu_i) \right] \tag{18}$$

$$\sigma_\theta = \lambda_i \left[A_i + \frac{B_i}{r^2} (1 - 2\nu_i) \right] \tag{19}$$

$$A_i = -\frac{r_i^2}{r_i^2 - r_a^2} \frac{p_i}{\lambda_i} \tag{20}$$

$$B_i = -\frac{r_i^2 r_a^2}{r_i^2 - r_a^2} \frac{p_i}{\lambda_i(1 - 2\nu_i)} \tag{21}$$

$$\lambda_i = \frac{E_i}{(1 - 2\nu_i)(1 + \nu_i)} \tag{22}$$

where E_i and ν_i are elastic Young's modulus and Poisson's ratio for the tube material and r_a is the internal radius of the tube.

The elastic, normal stiffness of the tube at $r = r_i$ is defined by

$$K_i = \frac{p_i}{U_{r=r_i}} = -\frac{\lambda_i(1 - 2\nu_i)(r_i^2 - r_a^2)}{r_i(r_i^2(1 - 2\nu_i) + r_a^2)} \tag{23}$$

For a solid inner tube (as in a rock bolt), $r_a = 0$ and equation (23) reduces to $K_i = -\lambda_i / r_i$.

Similarly, for an elastic outer tube of inner radius r_o, outer radius r_b, Youngs modulus, E_o and Poisson's ratio ν_o, the following equations are applicable:

$$U_r = A_o r + \frac{B_o}{r} \tag{24}$$

$$\sigma_r = \lambda_o \left[A_o - \frac{B_o}{r^2} (1 - 2\nu_o) \right] \tag{25}$$

$$\sigma_\theta = \lambda_o \left[A_o + \frac{B_o}{r^2} (1 - 2\nu_o) \right] \tag{26}$$

$$A_o = \frac{r_o^2}{r_b^2 - r_o^2} \frac{p_o}{\lambda_o} \tag{27}$$

$$B_o = \frac{r_o^2 r_b^2}{r_b^2 - r_o^2} \frac{p_o}{\lambda_o(1 - 2v_o)} \tag{28}$$

$$\lambda_o = \frac{E_o}{(1 - 2v_o)(1 + v_o)} \tag{29}$$

$$K_o = \frac{p_o}{U_{r=r_o}} = \frac{\lambda_o(1 - 2v_o)(r_b^2 - r_o^2)}{r_o(r_o^2(1 - 2v_o) + r_b^2)} \tag{30}$$

For an outer tube of infinite extent, i.e. a pile or anchor in a rock mass with an *in situ* stress of p_{og}, $r_b \to \infty$ and equations (27), (28) and (30) reduce to $A_o = 0$, $B_o = r_o^2(p_o - p_{og})/\lambda_o(1 - 2v_o)$ and $K_o = (\lambda_o/r_o)(1 - 2v)$.

By enforcing compatability of radial displacements at the inner and outer boundaries of the grout annulus, i.e. at $r = r_i$ and $r = r_o$ it is possible to determine the following equations for p_i and p_o:

$$p_i = \frac{2(1 + v_g) r_i K_i I_{r_i}^{r_o}}{r_o K_o \left[\dfrac{r_i K_i - \lambda_g(1 - 2v_g)}{r_o K_o - \lambda_g(1 - 2v_g)}\right]\left[\dfrac{r_o^2 K_o + r_o \lambda_g}{\lambda_g K_o}\right] - r_i^2 \left[\dfrac{r_i K_i + \lambda_g}{\lambda_g}\right]} \tag{31}$$

$$p_o = \frac{2(1 + v_g) r_o K_o I_{r_i}^{r_o} \left[\dfrac{r_i K_i - \lambda_g(1 - 2v)}{r_o K_o - \lambda_g(1 - 2v)}\right]}{r_o K_o \left[\dfrac{r_i K_i - \lambda_g(1 - 2v_g)}{r_o K_o - \lambda_g(1 - 2v_g)}\right]\left[\dfrac{r_o^2 K_o + r_o \lambda_g}{\lambda_g K_o}\right] - r_i^2 \left[\dfrac{r_i K_i + \lambda_g}{\lambda_g}\right]} \tag{32}$$

For a pile in rock, there is no inner boundary (i.e. $r_i = r_a = 0$) and equation (32) reduces to

$$p_o = \frac{2(1 + v_g)\lambda_g K_o I_0^{r_o}}{r_o(\lambda_g + K_o r_o)} \tag{33}$$

Yield at the inner boundary

For relatively low values of outer boundary stiffness, K_o tensile radial stresses, p_i, can be generated at the inner boundary of the grout. Low values of outer boundary stiffness allow the grout to expand radially outwards, pulling the inner boundary with it. In such cases it is unlikely that these tensile stresses can be sustained across the inner boundary resulting in the expansive grout separating from the inner tube. A tension cut-off can be included in the analysis, such that when p_i exceeds the given tensile strength, σ_t, the inner boundary stiffness is set to zero, i.e. for $p_i > \sigma_t$, $K_i = 0$.

If on the other hand K_o is relatively large, the grout will be forced to expand inwards against the inner stiffness, K_i, thereby generating compressive stresses on the inner boundary. This is unlikely to cause the inner tube to fail, unless the tube is very thin and buckling becomes a problem. The solution to this problem is beyond the scope of this paper.

Yield at the outer boundary

For the expansive grout applications discussed earlier, the outer boundary of the expanding grout annulus will either be an infinite rock mass (piles and anchors) or a metal tube (tubular

connections). If the strength of these confining materials is not adequate, the expanding grout may cause the outer boundary to yield. Yelding will cause a decrease in the outer stiffness, K_o. Equations for determining the value of K_o once yielding has occurred for three different situations are summarized below.

Case 1. *Elasto-plastic tube*: For simplicity, it is assumed that the outer tube is made from an elasto-perfectly plastic material with yield defined by the maximum shear stress or Tresca criterion. Yield will therefore occur when the maximum deviator stress, $(\sigma_r - \sigma_\theta)$, at any point in the tube reaches the yield strength of the tube σ_y. Equating with equations (25)–(29) results in the following equation for the external pressure, p_{oy}, required to intiate yield at the inner surface of the outer tube (i.e. at $r = r_o$).

$$p_{oy} = \sigma_y \frac{r_b^2 - r_o^2}{2r_b^2} \tag{34}$$

For pressures $p_o > p_{oy}$, the yield zone will extend further into the tube, and will form an annulus of yielded material of radius r_{oy}. By combining the equations for equilibrium and yield and enforcing the boundary condition at $r = r_o$, the following equations for the stresses within the yield zone can be determined:

$$\sigma_r = \sigma_y \ln\left(\frac{r}{r_o}\right) - p_{oy} \tag{35}$$

$$\sigma_\theta = \sigma_y \ln\left(\frac{r}{r_o}\right) + \sigma_y - p_{oy} \tag{36}$$

Enforcing the yield condition that at $r = r_{oy}$, $\sigma_r = -p_{oy}$, leads to the following equation for the radius of the yield zone:

$$\frac{r_{oy}}{r_o} = \exp\left(\frac{p_o - p_{oy}}{\sigma_y}\right) \tag{37}$$

By considering the change in volume of the yield zone and enforcing the condition of no volume change during yield, the radial displacement of the inner surface of the tube can be determined as

$$U_{r=r_o} = \frac{p_{oy}[(1-2\nu_o)r_{oy}^2 + r_b^2]r_{oy}^2}{\lambda_o(1-2\nu_o)(r_b^2 - r_{oy}^2)r_o} \tag{38}$$

The corresponding stiffness for a yielded outer tube is given by

$$K_o = \frac{p_o}{U_{r=r_{oi}}} = \frac{\lambda_o(1-2\nu_o)(r_b^2 - r_{oy}^2)r_o p_o}{r_{oy}^2((1-2\nu_o)r_{oy}^2 + r_b^2)\, p_{oy}} \tag{39}$$

A simple iterative procedure can be used to determine K_o and p_o from equations (32) and (39).

Case 2. *Elasto-plastic infinite rock mass*: A similar procedure to above can be adopted to determine the stiffness when the outer surface of the expanding grout cylinder is in contact with an elasto-plastic, homogeneous and isotropic rock mass with an *in situ* stress of p_{or}. It is assumed that the rock yields according to a Mohr–Coulomb failure criterion with cohesion, c_o, and internal friction angle, ϕ_o. The solution[4,5] adopts a non-associative flow rule[6] with a constant angle of dilation, ψ.

At an interface pressure of $p_o = p_{of} = c_o \cos\phi_o + p_{or}(1 + \sin\phi_o)$ a yield zone begins to form on the interface. For pressures in excess of p_{of} the yield zone extends into the rock mass, its radius r_{of} given by the following equation:

$$\frac{r_{of}}{r_o} = \left(\frac{p_o(m_o - 1) + \hat{\sigma}_o}{p_{of}(m_o - 1) + \hat{\sigma}_o}\right)^{m_o/(m_o - 1)} \tag{40}$$

where

$$m_o = \frac{1 + \sin\phi_o}{1 - \sin\phi_o} \quad \text{and} \quad \hat{\sigma}_o = \frac{2c_o \cos\phi_o}{1 - \sin\phi_o}$$

As a result, the stiffness of the rock mass reduces to

$$K_o = \frac{p_o \lambda_o (1 - 2v_o)}{r_o\left(b_{o1}\left(\frac{r_{of}}{r_o}\right)^{(m_o - 1)/m_o} + b_{o2}\left(\frac{r_{of}}{r_o}\right)^{(n_o + 1)/n_o} + b_{o3}\right)} \tag{41}$$

where

$$b_{o1} = \frac{-2m_o}{m_o - 1}\left((1 - v_o)\frac{(1 + m_o n_o)}{(m_o + n_o)} - v_o\right)(p_{of} - p_{or}), \qquad b_{o2} = 2n_o(1 - v_o)\frac{(m_o + 1)}{(m_o + n_o)}(p_{of} - p_{or}),$$

$$b_{o3} = (1 - 2v_o)\frac{(m_o + 1)}{(m_o - 1)}(p_{of} - p_{or}) \quad \text{and} \quad n_o = \frac{1 + \sin\psi_o}{1 - \sin\psi_o}$$

As with Case 1, a simple iterative procedure can be used to determine K_o and p_o from equations (33) and (41).

Case 3. *Brittle or jointed rock mass*: Several investigators[7–12] have investigated the expansion of cylindrical cavities in rock. They argued that the expansion may cause radial cracking to occur prior to any yielding or crushing of the rock. Haberfield and Johnston[11] argued that the pressure, p_{oc}, at which these cracks develop depends on the tensile strength, $|\sigma_{ot}|$, of the rock and the *in situ* horizontal stress, p_{or}, and is given by $p_{oc} = 2p_{or} + |\sigma_{ot}|$. They further proposed that radial cracking could only occur if $p_{oc} < p_{of}$. That is if $|\sigma_{ot}| < c_o \cos\phi_o - p_{or}(1 - \sin\phi_o)$.

Assuming that $p_{oc} < p_{of}$, then for values of $p_o > p_{oc}$, the cracks will propagate further into the rock mass causing a reduction in stiffness. Using fracture mechanics theory to govern crack propagation, Haberfield and Johnston[13] developed a finite element program to model the cracked response. Predictions from the finite element program were found to be in good agreement with laboratory tests.[11] From the results of the finite element analyses they[12] were able to determine the following empirical relationship between the length of the propagating crack and the interface pressure, p_o, for cavity expansions in weak siltstone:

$$\frac{r_{oc}}{r_o} = 3\left(\frac{p_o}{p_{oc}} - 1\right) \times 10^{-1{\cdot}88 p_{og}/p_{oc}} + 1 \tag{42}$$

It should be noted that this relationship may not be appropriate for other rocks. The stiffness of the cavity is determined from the elastic solution given earlier for $p_o < p_{oc}$ and from equation (43)

for $p_{oc} \leqslant p_o \leqslant q_{uo}$ where q_{uo} is the uniaxial strength of the rock:[12]

$$K_o = \frac{(1 - 2v_o)\lambda_o}{r_o((1 - v_o)\ln(r_{oc}/r_o) + 1 - p_{or}r_{oc}/p_o r_o)} \tag{43}$$

Since propagation of radial cracks releases the tensile circumferential stresses, the rock wedges between the cracks are essentially loaded in uniaxial compression. The response of these rock wedges will remain elastic until the uniaxial strength of the rock, q_{uo}, is reached. For $p_o > q_{uo}$ the rock between the cracks will crush and dilate and as a result, the cracks in this crushed zone will close, re-confining the rock once again in the circumferential direction. Unfortunately, due to the complexity of the processes involved, an appropriate analytical solution to this problem (for $p_o > q_{uo}$) could not be found.

The author[12] also used the finite element model mentioned above to determine the effect that joints, which intersect the cavity, have on the performance of the expanding cavity. Both uncemented and cemented joints were investigated. Near vertical joints were found to have essentially the same influence on the response as radial cracking (independent of the degree of cementation). On the other hand, horizontal joints had little influence and a response similar to the intact response was obtained. Other joint geometries have not been investigated, but it is likely that the response of the cavity will lie somewhere between the intact response and the radial cracked response. It follows then for a rock mass containing near vertical joints that intersect the cavity (and in which $p_{oc} < p_{of}$), equations (42) and (43) should be used to determine stiffness. For uncemented joints a uniaxial tensile strength of zero should be adopted. For all other cases, the equations determined for Case 2 should be adopted.

DETERMINATION OF EXPANSIVE POTENTIAL

From the equations listed above, it is clear that the stiffness of the material confining the expanding grout cylinder has a large affect on the degree of expansion that takes place and on the normal stress developed. However, in order to use these equations to estimate the normal stress, the strain due to expansion, ε^E, needs to be determined. Unfortunately, ε^E is not constant but depends on expansive cement type and content, mix design, stress level and curing conditions.

To enable ε^E to be quantified, a series of laboratory tests were carried out. These tests, which are described in detail by Baycan,[14] made use of a standard soil oedometer rig. All tests were carried out using an expansive cement known as Denka CSA. Denka CSA is a Class C expansive cement which provides expansion through the formation of ettringite crystals. Four expansive paste mixes were tested. In each mix, a specified amount of CSA was added to normal cement and then mixed with water. The four mixes all used a water/total cement ratio of 0·45 and had CSA to total cement ratios (CSA^r) of either 0, 0·069, 0·138 or 0·207.

Immediately after mixing, the cement paste was placed into a standard steel oedometer ring with inner diameter of 75 mm, outer diameter of 80 mm and a height of 20 mm. The samples were then left for 2 h to become firm. Filter paper and porous stones were then placed on the top and bottom of samples (see Figure 5) and the sample placed into the oedometer rig. A specified constant preload was then applied to the sample, and measurements of vertical displacement were taken using very accurate dial gauges, at regular intervals over the next 30 days. At all times, the sample was immersed in water; the porous stones and filter paper providing a conduit for water to the top and bottom of the samples. Preloads ranged between 100 and 2500 kPa.

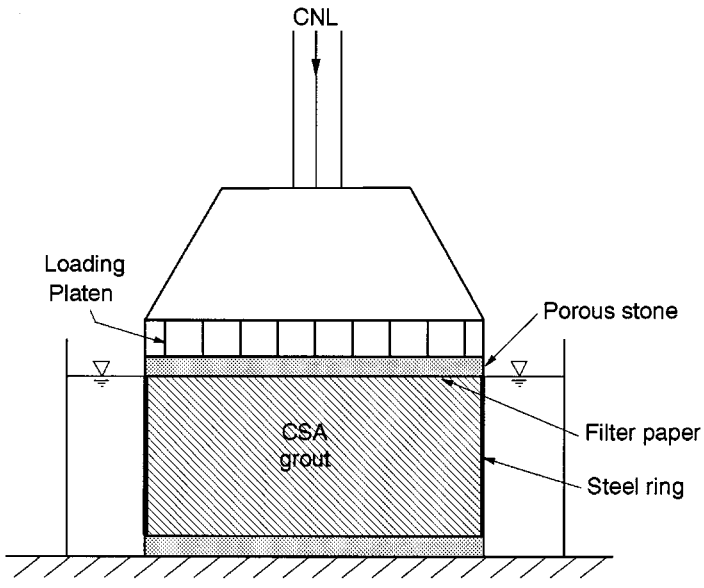

Figure 5. Determination of expansive grout performance using a soil oedometer apparatus

Since the oedometer ring is relatively stiff, expansion is forced to occur in the vertical direction. Analysis of the test set-up using analytical solutions similar to those given earlier, show that the finite stiffness of the oedometer ring has a negligible effect on the vertical expansion of the grout and can be ignored. Typical plots of vertical expansion versus time obtained from the oedometer tests are shown in Figure 6. Figure 6(a) compares expansion vs. time plots for the four different mixes all at a preload of 1500 kPa, while Figure 6(b) compares curves for a $\mathrm{CSA}^{\mathrm{r}} = 0{\cdot}138$ mix at several different preloads. Figure 6 clearly shows the dependence of expansion on preload and CSA content. It is worth noting that all expansion ceases after an initial period of 5–20 days. The time taken for the expansion process to occur, appears to depend on the normal stress applied and the CSA content. Greater CSA contents and higher normal stresses require a longer time for completion of the expansion process.

The maximum expansion from each test, expressed in terms of strain, is plotted against applied normal stress in Figure 7. In each case, a small correction (based on a measured Young's modulus for the grout of 5000 MPa) to the strain has been made to account for the elastic displacement of the sample resulting from the applied normal stress. Using standard curve-fitting procedures, the following empirical equation to describe the variation of expansive strain, ε^{E}, with expansive cement content, $\mathrm{CSA}^{\mathrm{r}}$, and normal stress ratio, $\bar{\sigma}_{\mathrm{n}}$ has been determined:

$$\varepsilon^{\mathrm{E}} = \left(\frac{\mathrm{CSA}^{\mathrm{r}}}{0{\cdot}006\bar{\sigma}_{\mathrm{n}} + 0{\cdot}33} \right)^4 \tag{44}$$

where $\bar{\sigma}_{\mathrm{n}} = \sigma_{\mathrm{n}}/p_{\mathrm{a}}$ and σ_{n} is the applied normal stress and p_{a} is atmospheric pressure, taken to be 100 kPa in this case. The resulting curves for the four paste mixes are also included in Figure 7

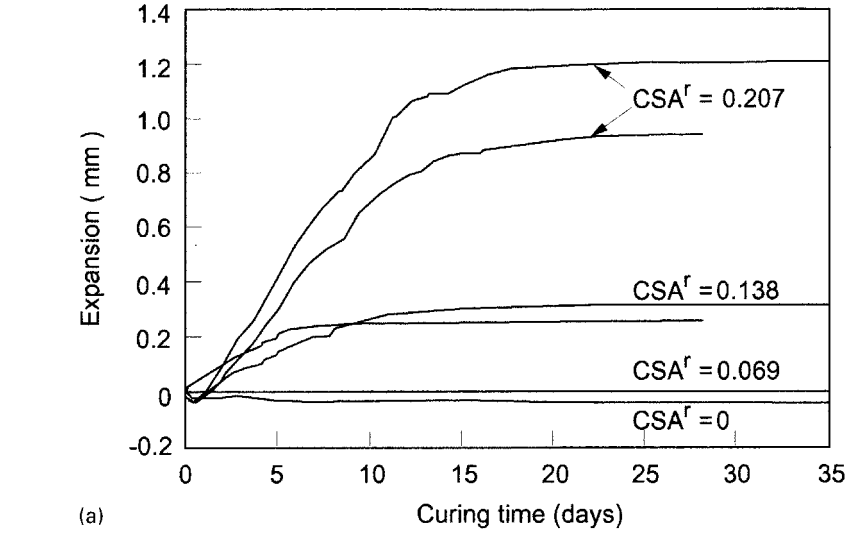

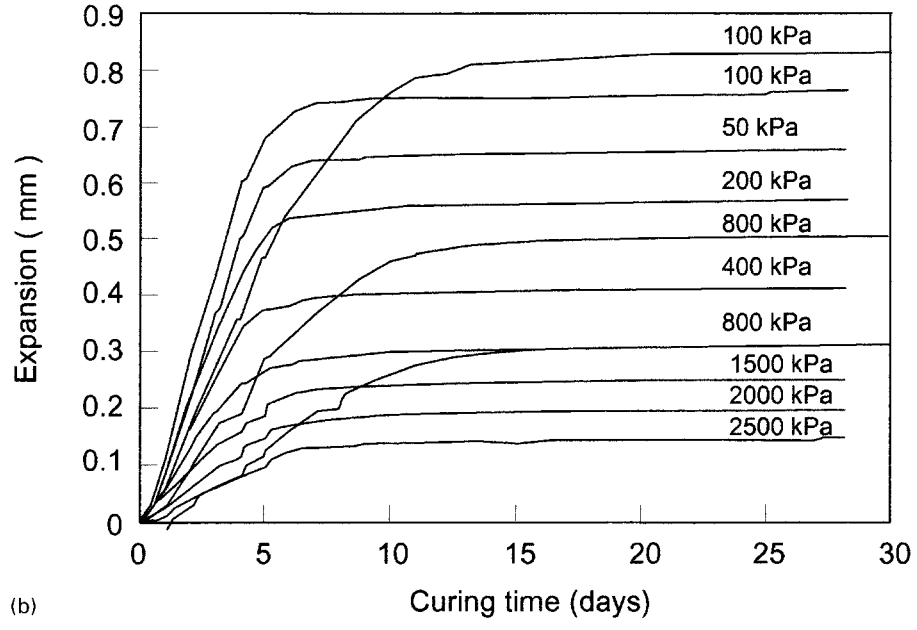

Figure 6. Results of oedometer tests on expansive grout: (a) expansion versus time plots for different CSA contents (normal stress = 1500 kPa); (b) expansion versus time plots for different normal stresses ($CSA^r = 0{\cdot}138$)

(note that the curves for $CSA^r = 0{\cdot}0$ and $0{\cdot}069$ plot on or near the horizontal axis). A good fit to the experimental data has been obtained.

It should be emphasized that equation (44) has been determined for cement pastes made from Denka CSA, normal cement and water and cured under near ideal conditions. The use of other

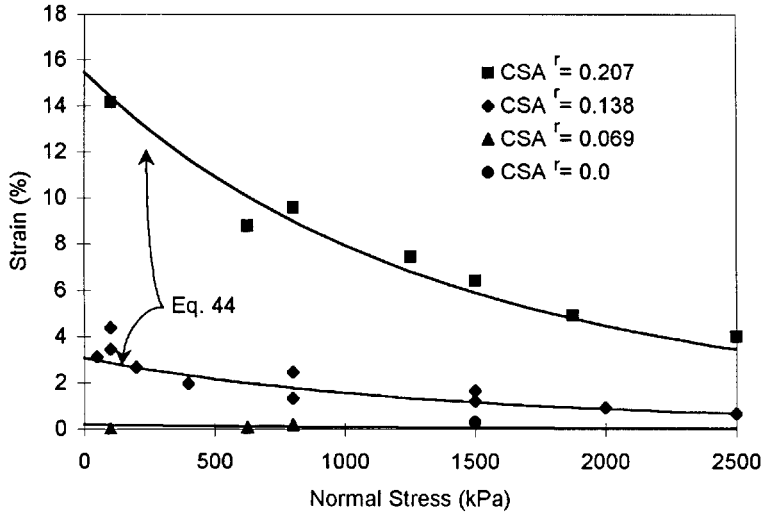

Figure 7. Maximum expansive strain versus applied normal stress for a range of CSA contents

types of Class C expansive cements, other mix designs or different curing conditions are likely to result in a different relationship than that given by equation (44). Nevertheless, the same procedure as described here (using standard oedometer rigs) can be used to establish a similar relationship for any type of expansive cement and for any mix design. Preliminary studies carried out by the author have indicated that concrete mixes which adopt the same weight of CSA per cubic metre of concrete as the cement paste mixes described here, give very similar expansions to those predicted by equation (44). Research in this area is continuing.

The amount of expansion also depends on the curing conditions. In particular, the amount of free water available for the cement hydration process governs the amount of ettringite formed. Hence, full expansion potential may not be realized if there is not enough free water available. In such cases, equation (44) will overpredict the amount of expansion.

COMPARISON WITH LABORATORY CONFINED EXPANSION TESTS

A number of confined expansion tests were carried out in the laboratory to test the accuracy of the thermal model of expansion derived earlier. These tests involved casting cement paste into tubes and then measuring the expansion of the tubes until expansion ceased. The expansion of the tubes was measured using strain gauges glued to the outside surface of the tubes at mid-height. These tests utilized the same four cement paste mixes that were used in the oedometer tests. The tubes remained completely immersed in water at 20°C throughout testing.

All confining tubes had length to diameter ratios of 2:1 and ranged in stiffness from 3·2 to 1665 MPa/mm. The range in stiffnesses was made possible by using tubes of different material, diameter and wall thickness. The tubes were made from either steel, aluminium and PVC. The aluminium tubes were coated with epoxy resin to minimize any expansive reaction between the aluminium tube and the cement. Tube stiffnesses were initially determined from equation (30),

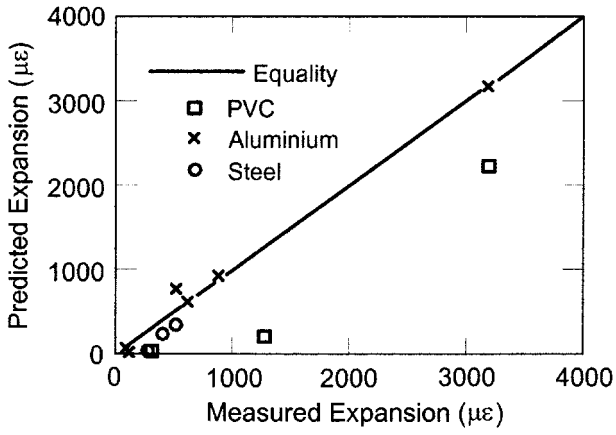

Figure 8. Predicted versus measured expansion for confined cylindrical samples of expansive grout

and then confirmed through pressure vessel testing.* The tubes showed similar expansion time responses to those observed in the oedometer tests. Full details of these tests are provided in Reference 14.

Figure 8 compares measured and predicted values of peak circumferential strain as determined on the outside surface of the confining tubes. Figure 9 shows the estimated variation of induced normal stress with CSA content and tube stiffness. The expansive grout response was determined from equations (8)–(16) and the confining tube behaviour by equations (25)–(30). The normal stress was determined from equation (33). In some cases, the expansive paste caused the confining tube to yield,† and hence equations (34)–(39) replaced equations (8)–(16) for determination of confining tube behaviour. Equation (44) was used to estimate the expansive strain. Note that since the expansive strain (equation (44)) is dependent on the stress, which in turn is dependent on how much expansion occurs, an iterative procedure must be adopted to obtain a solution. To start the procedure an initial value of $\sigma_n = 0$ can be assumed. Convergence in all cases is rapid. The predictions were made using the parameters listed in Table I. The yield strength values were determined from tensile strength tests of the tubes, and the Young modulus values back calculated from the pressure vessel tests.

In general, reasonable predictions have been obtained. However, for the PVC tubes the theoretical model underestimates expansion. The main reason for the underestimation is that the PVC tubes were found to creep excessively during the test, and therefore the elastic plastic model adopted in the analytical solution was not appropriate.

FIELD TESTING OF ROCK ANCHORS

As part of a larger investigation into the use of expansive cements in geotechnical applications, 12 anchors were grouted into a moderately weathered siltstone. The purpose of the tests was to

* These tests involved constructing pressure vessels with a length to diameter ratio 4:1 from the tubes. The pressure vessels were strain gauged and then pressurized using compressed air and water. The stiffness was determined from the slope of the circumfrential strain vs. pressure curve

† The stiffness values cited in Table I are elastic values and do not take into account the yielding of the tube

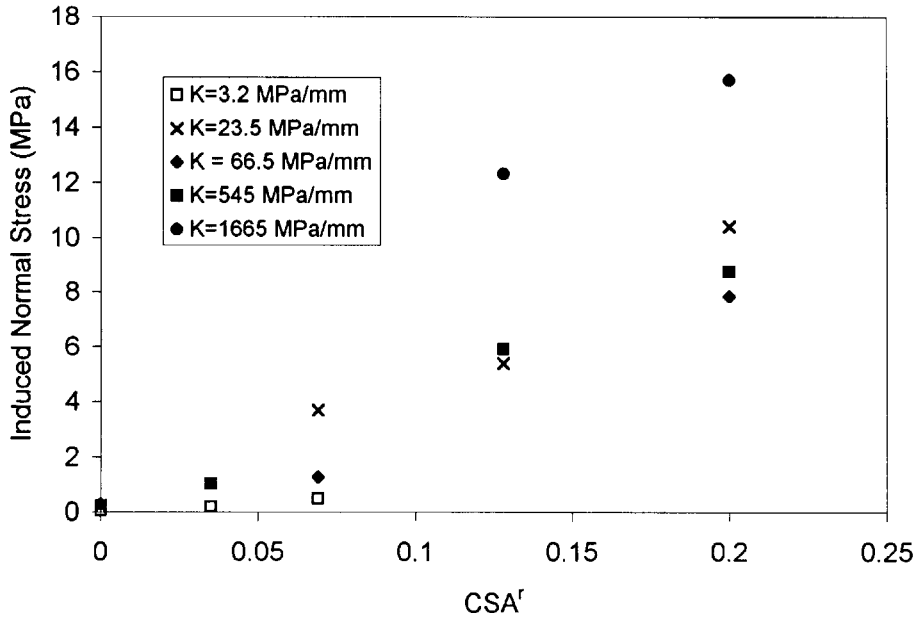

Figure 9. Variation of induced normal stress with CSA content and confining tube stiffness as determined from confined cylinder tests

Table I. Parameters used for model predictions

Confining tube			E	ν	Yield strength
r_o (mm)	r_b (mm)	K_o (MPa/mm)	(MPa)		(MPa)
42·5	44·5	3·2	$6{\cdot}9 \times 10^4$	0·3	
98·5	101·5	23·5	$6{\cdot}9 \times 10^4$	0·34	230
47·5	49·5	66·5	$6{\cdot}9 \times 10^4$	0·34	230
16·0	18·0	545	$6{\cdot}9 \times 10^4$	0·34	230
24·0	29·0	1665	$2{\cdot}1 \times 10^5$	0·3	350
		Concrete	$2{\cdot}6 \times 10^4$	0·15	
		Grout	$1{\cdot}0 \times 10^4$	0·2	

determine the variation in anchor capacity with initial normal stress level by changing the quantity of expansive cement in the grout mix. The grout used in the field anchors was identical to that used in the laboratory expansion tests described immediately above. Extensive sampling and testing of the siltstone was carried out to determine engineering properties. Tests included uniaxial compression tests, drained triaxial tests, Brazilian tests and insitu pressuremeter tests. The siltstone was found to be relatively uniform with a uniaxial compressive strength of approximately 5 MPa. The 98 mm diameter anchor holes were drilled with a percussion hammer

drill using a 210D Gemco rig operated with an on-site air compressor unit. The surface roughness of the boreholes was measured using a purpose-made down-hole roughness measuring device developed by Baycan.[14] To ensure that failure occurred on the grout–rock interface (rather than at the tendon–grout interface or by tendon failure), the bonded length of the anchor was restricted to 250 mm. Full details of the anchor tests can be found in Reference 14.

Typical load displacement responses for the anchors are shown in Figure 10. Anchor capacity has been plotted in terms of shaft resistance (total axial force divided by bonded surface area of anchor). The increase in capacity with CSA^r is clearly demonstrated. Using the theoretical equations developed earlier and assuming the properties of the siltstone listed in Table I,[14] estimates of the initial normal stress generated by the different values of CSA^r were made. Using these values it is possible to develop a strength envelope for the anchor–rock interface as shown in Figure 11. Figure 11 plots the ultimate anchor capacity on the vertical axis (shear stress) against estimated initial normal stress on the horizontal axis. The initial normal stress is the normal stress induced by the expansive cement and excludes any extra normal stress generated during anchor pull out. Values were estimated using the procedures described earlier in the paper. A line of best fit has been fitted to the data using linear regression and ignoring the two high values at approximately $\sigma_o = 2$ and 7 MPa. The line has an intercept of 3·66 MPa and a slope of 30·5°. If it is assumed that the linear Mohr–Coulomb failure criteria can be used to represent the strength of the grout–rock interface, then it is possible to determine the adhesive and frictional components of strength from this best-fit line. The adhesion is determined from the intercept and most likely arises from the cementation that has developed between the cement grout and the rock. The slope, on the other hand, defines the frictional component of resistance, and is dependent on the normal stress on the grout–rock interface. The regression line indicates a friction angle of 30·5°.

Independent analyses of anchor resistance based on surface roughness measurements and theory developed by Seidel and Haberfield[15] indicates a friction angle of between 30 and 32° for

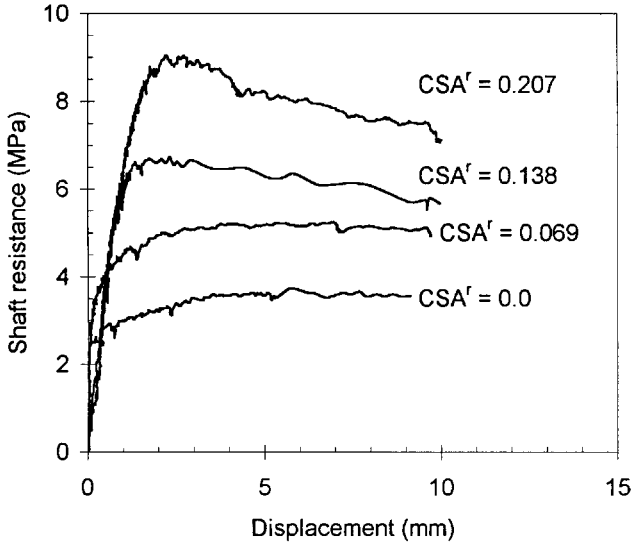

Figure 10. Typical load deformation responses for rock anchors with different CSA^r values

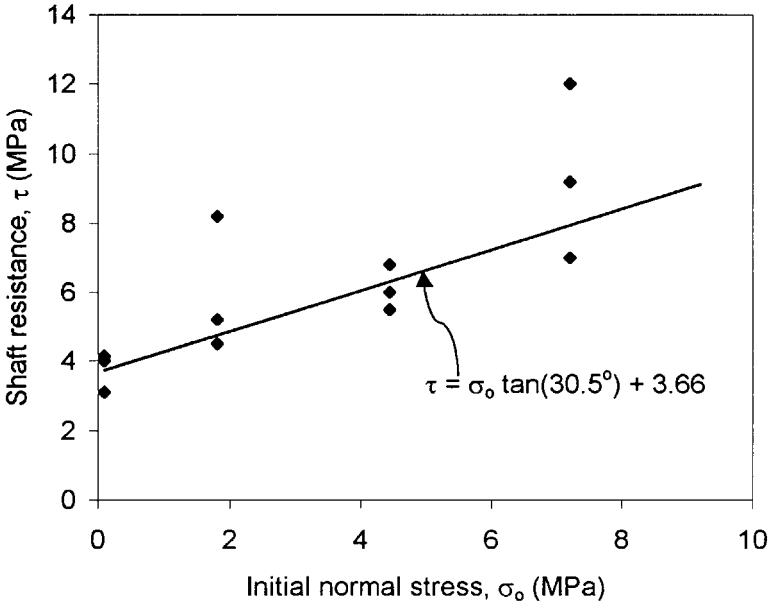

Figure 11. Anchor–rock interface strength envelope

the grout–rock interface. Laboratory constant normal stiffness direct shear tests on grout–siltstone interfaces with similar surface roughnesses to those measured in the anchor holes[14] also returned peak friction angles in this range. Both estimates are in good agreement with the empirically determined value of 30·5°.

From these analyses it appears that the analytical model of expansion can be used to estimate the increase in anchor resistance obtained by using expansive cements. However, it should be emphasized that the results have only been tested for anchors in one type of rock with relatively smooth borehole roughness. In such cases, the normal stress generated during anchor pullout is relatively low and the initial normal stress dominates performance. However, as roughness level increases, the normal stress generated during anchor pullout increases significantly, and can thereby reduce the impact of the initial normal stress. For such conditions, the simple linear Mohr–Coulomb model applied above is no longer appropriate. Work in this area is continuing.

APPLICATION TO PILES IN ROCK

It is of some interest to investigate the range of possible initial normal stresses that can be generated in piles socketed into rock. With such knowledge it is possible to estimate the likely load displacement performance of the piles[15] and thereby optimize the quantity of expansive cement. Typical pile diameters and rock properties, in combination with the equations and procedures described earlier, have been used to generate the results shown in Figure 12. Figure 12(a) plots the initial normal stress induced from concrete expansion against the uniaxial compressive strength of the rock, for three different CSA contents. The dashed line indicates the normal stress required to initiate failure in the rock mass. Figure 12(b) shows the corresponding

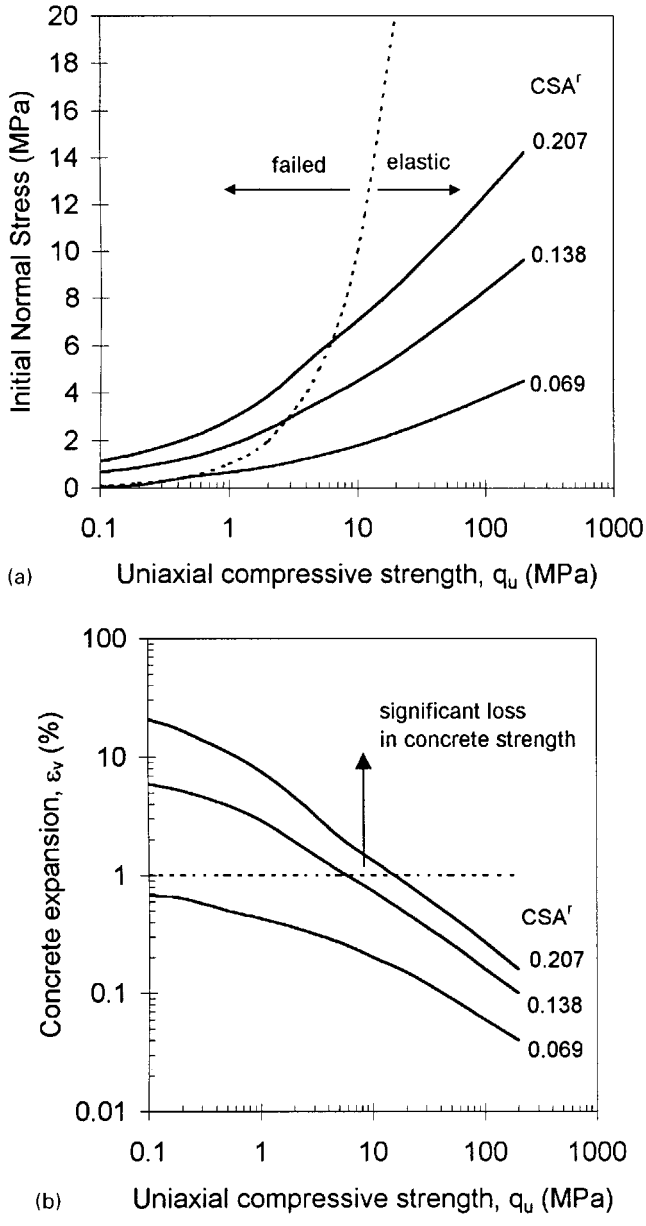

Figure 12. Predicted response of expansive concrete piles socketed into rock: (a) expected variation in initial normal stress with rock strength; (b) corresponding expected concrete expansion with rock strength

amount of concrete expansion (in % volume) which is expected to occur. In rocks of relatively low strength and therefore stiffness, high expansions occur, but only relatively low initial normal stresses are generated. As demonstrated by Chamberlain,[16] volume expansions in excess of approximately 1 per cent under unconfined conditions result in a significant loss of concrete

strength. Although this strength reduction will be less under confined conditions, high concentrations of expansive additive under low confinement conditions should be avoided until more testing is carried out. For high stiffnesses, little if any expansion can occur, and the initial normal stress developed can be significant and can cause yielding of the surrounding rock. This can ultimately lead to higher than expected expansions and some decrease in concrete strength. However, for cases in which high initial normal stresses are generated and expansions remain small, a significant increase in concrete strength is likely.

As stated earlier, the likely increase in pile capacity resulting from the addition of expansive additive will depend on the relative roughness of the pile socket. For smooth sockets, an increase in CSA^r is likely to result in a significant increase in pile capacity (assuming the confinement is sufficient). However, for rough sockets the relationship between CSA^r and pile capacity is unlikely to be straightforward, and the increase in capacity may be somewhat reduced.

SUMMARY

A thermal expansion analogy has been used to model the behaviour of expansive grout under confined situations. Through this simple model, equations have been developed to estimate the degree of expansion and the initial normal stresses that can be generated in some relatively promising applications of expansive cement, e.g. piles and anchors in rock and tubular connections. The model relies on the estimation of the expansive potential, which can be estimated using a relatively simple laboratory test. Expansive potential has been found to vary with expansive cement content and confining stress level, but probably also depends on expansive cement type, grout mix design and the amount of free water available during hydration. An empirical equation relating expansive potential to expansive cement content and stress level has been determined for cement paste made from ordinary portland cement and Denka CSA. Further testing is required to establish appropriate relationships for other expansive cements and for grouts and concretes.

Predictions from the analytical model were compared with results from laboratory tests on confined cylinders of expansive grout and from field rock anchor tests. In both cases reasonable agreement between measured and predicted results were obtained.

ACKNOWLEDGEMENTS

The research described in this paper was funded by the Australian Research Council. Their support is gratefully acknowledged.

REFERENCES

1. C. M. Haberfield, T. Chamberlain and S. Baycan, 'Aspects of using expansive concretes to improve drilled pier performance in weak rock', *Proc. Int. Conf. on Design and Construction of Deep Foundations*, Orlando, FL, December 1994, pp. 631–645.
2. M. W. O'Neill, K. H. Hassan and S. A. Sheikh, 'Bored piles in clay-shale using expansive concrete', in Van Impe (ed.), *Proc. Int. Seminar on Deep Foundations and Auger Piles*', Balkema, Rotterdam, June 1993, pp. 289–294.
3. P. Grundy and J. E. O. Foo, 'Prestress enhancement of grouted pile/sleeve connections', *Proc. Int. Soc. of Offshore and Polar Engineering ISOPE'91*, Edinburgh, August 1991, pp. 130–136.
4. P. Fritz, 'An analytical solution for axisymmetric tunnel problems in elasto-viscoplastic media', *Int. J. Numer. Analyt. Meth. Geomech.*, **8,** 325–342 (1984).
5. J. P. Carter, J. R. Booker and S. K. Yeung, 'Cavity expansions in cohesive frictional soils', *Geotechnique*, **36**(3)**,** 349–358.

6. E. H. Davis, 'Theories of plasticity and the failure of soil masses', in I. K. Lee (ed.), *Soil Mechanics Selected Topics*, Butterworths, London, 1968, pp. 341–380.
7. M. Rocha, A. De Silveria, N. Gossman and E. De Oliveira, 'Determination of the deformability of rock masses along boreholes', *Proc. 1st Int. Cong. on Rock Mech.*, Lisbon, Vol. **1,** 1966, pp. 697–704.
8. B. Ladanyi, 'Expansion of cavities in brittle media', *Int. J. Rock Mech. Min. Sci.*, **4,** 301–328 (1967).
9. B. Ladanyi, 'Quasi-static expansion of a cylindrical cavity in rock', *Proc. 3rd Symp. on Engineering Applications of Solid Mechanics*, Toronto, Vol. 2, 1976, pp. 219–240.
10. B. Ladanyi, 'A lower-bound solution for bursting of thick-walled cylinders of rock under internal and external pressures', Structure et comportment mecanique des geomateriaux, Colloque Rene Houpert, Nancy, 10–11 September 1992, pp. 269–279.
11. C. M. Haberfield and I. W. Johnston, 'Model studies of pressuremeter testing in soft rock', *ASTM Geotech. Testing J.*, **12**(2)**,** 150–156 (1989).
12. C. M. Haberfield, 'The performance of the pressuremeter and socketed piles in weak rock', *Ph.D. Thesis*, Monash University, Melbourne, 1987.
13. C. M. Haberfield and I. W. Johnston, 'A numerical model for pressuremeter testing in weak rock', *Geotechnique*, **40,** 569–580 (1990).
14. S. Baycan, 'Field performance of expansive anchors and piles in rock', *Ph.D. Dissertation*, Department of Civil Engineering, Monash University, 1997.
15. J. P. Seidel and C. M. Haberfield, 'The shear behaviour of concrete-soft rock joints. Part 3—drilled shafts in rock', *Departmental Report*, Department of Civil Engineering, Monash University, Australia, 1997.
16. T. D. Chamberlain, 'Investigation of expansive cements and their influence on the capacity of socketed piles and grouted anchors in rock', *MEngSc* (Research) *Dissertation*, Department of Civil Engineering, Monash University, 1993.

